

Hydrogen Elimination Kinetics during Chemical Vapor Deposition of Silica Films

F. Ojeda,^{†,‡} F. Abel,[§] and J. M. Albella^{*,‡}

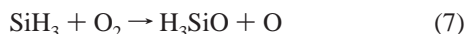
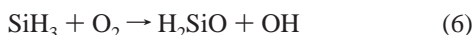
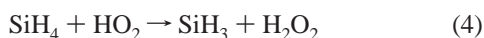
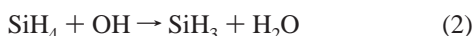
Departamento de Física e Ingeniería de Superficies, Instituto de Ciencia de Materiales de Madrid (CSIC), Cantoblanco, 28049 Madrid, Spain, and Groupe de Physique des Solides, Universités Paris 7 et Paris 6, 2 Place Jussieu, 75251 Paris Cedex 05, France

Received: January 24, 2002; In Final Form: April 19, 2002

Hydrogen elimination mechanisms involved in the low-pressure chemical vapor deposition of silica films from SiH₄/O₂/N₂ mixtures are investigated. The main purpose of this work is to elucidate the mechanisms that limit hydrogen elimination in the silica deposition process under the mass-transport and gas-phase kinetic regimes. To this end, different gas-phase, surface, and mass-diffusion processes relevant to the SiH₄ oxidation and silica growth chemistry are considered and discussed on the basis of the influence of temperature, total gas flow rate and O₂-to-SiH₄ flow ratio on deposition rate and hydrogen content in the film, as determined by infrared spectroscopy and elastic recoil detection analysis. Our results indicate a clear relationship between the growth and hydrogen elimination kinetics, and support a hydrogen elimination model based on radical-surface interactions.

Introduction

Silicon oxides films deposited from thermally activated SiH₄/O₂ mixtures are commonly used as intermetal insulator, passivation layer, and diffusion barrier in the manufacture of silicon and II–VI/III–V semiconductor-based electronic devices.^{1–4} The most advantageous characteristic of the SiH₄/O₂ chemical vapor deposition (CVD) technique is the possibility of obtaining reasonably high deposition rates at very low temperatures (typically in the 300–450 °C range). At present, there is little question that this characteristic is due to the abundant formation of highly reactive free radicals through a branching-chain process in which SiH₄ molecules are attacked by H, O, OH, and HO₂ radicals (active chain carriers), yielding SiH₃ species (reactions 1–4) that ensure the chain feedback through different oxidation channels (reactions 5–7):



This set of primary reactions branches out through the HSiOOH, H₂SiO, and H₃SiO species into a series of secondary reaction steps, not fully understood to date, yielding silica film precursor species with the general formula SiO_mH_n, silica powder precursor species, byproducts (H₂, H₂O, and H₂O₂) and

active chain carriers (H, O, OH, and HO₂). The heterogeneous and homogeneous quenching of the chain carriers, and even of the SiH₃ species, determines the lower and upper critical ignition limits of silane oxidation, respectively. These schemes are consistent with the observed stoichiometry of SiH₄/O₂ explosions,⁵ ignition limits of silane oxidation,⁶ and chromatography measurements and photoemission spectra of silane/oxygen flames.⁷

Previous kinetic studies^{8–15} indicate that silica growth from the SiH₄/O₂ reaction proceeds predominantly through SiO_mH_n intermediate species formed in the gas phase, with negligible contribution of surface reactions between SiH₄ and O₂ molecules. The low gas-phase concentration of the SiO_mH_n species and their short lifetime make direct experimental observations a very difficult task, which explains the scarce number of studies dealing with this problem. Using in situ mass spectrometry, Liehr and Cohen¹² detected H_nSiO species (with $n \geq 1$) in pure SiH₄/O₂ mixtures at very low pressures (10⁻³ Torr). Van de Weijer and Zwerver¹⁴ reported the observation of SiO radicals in the gas phase by laser-induced fluorescence (LIF) during the thermal deposition of silica films from pure SiH₄/O₂ mixtures at 0.97 Torr. However, the chemical identity of the SiO_mH_n precursor species and the chemical mechanisms through which they are produced remains unsolved to date. What is known is that a certain amount of these hydrogenated species are trapped by the growing oxide without being completely dehydrogenated, leading to nonnegligible concentrations of OH and SiH groups incorporated in the film bulk. In this sense, silica growth involves a parallel hydrogen elimination process by which SiH₄ molecules contributing to film deposition lose most of their H atoms.

Noneliminated OH and SiH groups are one the main reasons for the degradation and failure of SiO₂-based solid-state devices. Nonbridging SiOH and SiH groups break the network continuity, resulting in porous structures and defects into the oxide matrix and thus in poor electrical, barrier, protective, and optical properties.^{12,16–23} In silica CVD, including SiH₄/O₂ CVD, hydrogen elimination is commonly enhanced by increasing temperature or the oxidant-to-hydride ratio in the gas mixture or by decreasing deposition rate or total pressure.^{9,12,20} Apart

* To whom correspondence should be addressed. Phone: 34 91 3349080. Fax: 34 91 3720623. E-mail: albella@icmm.csic.es.

[†] Present address: Technological & Business Development, Non-Destructive Testing, Tecnatom S.A., Avda. Montes de Oca, 1, 28709 San Sebastián de los Reyes, Madrid, Spain. Phone: 34 91 659 8659. E-mail: fojeda@tecnatom.es.

[‡] Instituto de Ciencia de Materiales de Madrid (CSIC).

[§] Universités Paris 7 et Paris 6.

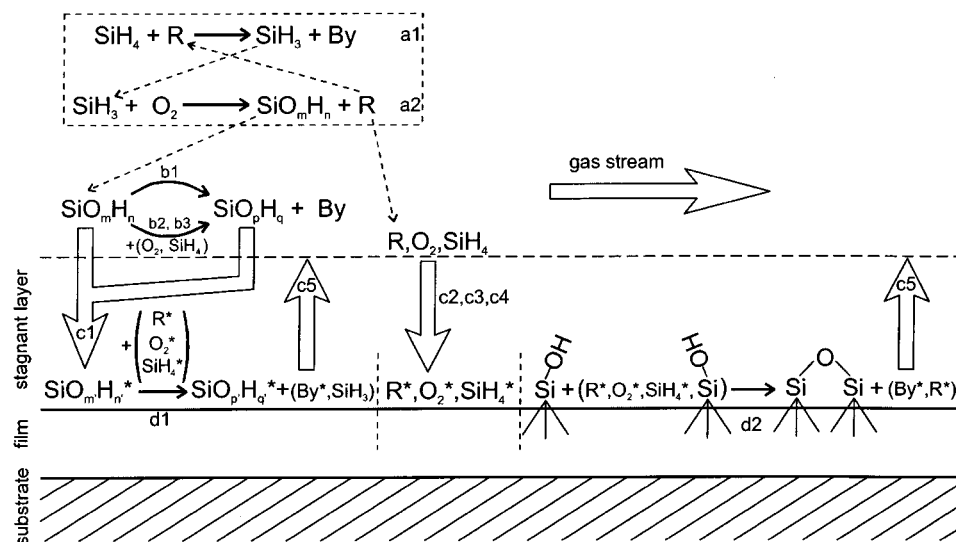


Figure 1. Growth and hydrogen elimination mechanisms relevant to the SiH_4/O_2 CVD system.

from the fact that these empirical methods do not always provoke the desired effect, little is known about the mechanisms causing and limiting hydrogen elimination during the CVD process, as well as about their connection with the film growth kinetics and the chemical paths involved in this process.

In a recent paper we have reported the influence of hydrogen incorporation on the structure and stoichiometry of silica films grown by SiH_4/O_2 CVD.²⁴ The present work focuses on a kinetic analysis of the mechanisms that limit hydrogen elimination during this deposition process under mass-transport and reaction-rate limited growth regimes. To this end, we have analyzed jointly the influence of the experimental parameters on deposition rate and hydrogen concentration in the film. Different hydrogen elimination mechanisms, occurring both in the gas phase and at the film surface, are discussed on the basis of our experimental observations. This study provides, on one hand, general methods useful to minimize and control the hydrogen content in the film and, on the other hand, analysis criteria to study the hydrogen elimination kinetics in other deposition processes.

Experimental Section

Hydrogenated silica thin films were chemically vapor deposited on monocrystalline (100) oriented silicon wafers (Virginia Semiconductors) polished on both faces. The deposition system was a low-pressure hot-wall horizontal CVD reactor described elsewhere.¹⁵ This reactor was fabricated from a quartz tube with an inner diameter of 6.1 cm and a total length of 100 cm. The length of the heating zone, which is centered in a 30 cm long cylindrical furnace, is 10 cm. A horizontal graphite plate was used as substrate-holder. The flow of the reactants, SiH_4 (diluted at 2% in N_2 , 99.999% purity) and O_2 (99.9992% purity), was adjusted by means of mass flow controllers. To prevent gas-phase reactions in the front zone of the tube, silane was separately introduced through a stainless steel injector up to the entrance of the reaction zone. Low-pressure conditions were achieved by means of a vacuum system that consists of a rotary pump boosted by a Roots pump. The base pressure, as measured by a Penning gauge, was 5×10^{-4} Torr. The process pressure was measured by a capacitive gauge and controlled by means of an electronically driven throttle valve. The deposition rate was estimated from thickness measurements obtained by means of a profilometer (Dektak 3030).

IRS (infrared spectroscopy) was employed to study *ex situ* the hydrogen concentration incorporated in the films. IR-

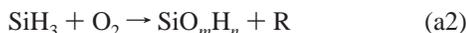
transmittance spectra were recorded using a double-beam dispersive spectrophotometer (Hitachi 270-50) in normal incidence mode. The OH:SiOSi bond ratio in the film was obtained from the ratio between the areas behind the O–H and Si–O–Si stretching absorbance bands (found at 3760 and 1070 cm^{-1} , respectively), according to the procedure described elsewhere.²⁴ The stretching Si–H absorption band, typically located at 2250 cm^{-1} in silica,²⁵ was always absent in our IR spectra. Therefore, the OH:SiOSi ratio (accounting for both SiOH and H_2O species) was considered to be a good measure of the total hydrogen concentration incorporated in the film.²⁴

Hydrogen depth profiles across the silica films were obtained by ERDA (elastic recoil detection analysis) in the 2.5 MeV Van de Graaf accelerator at the Groupe de Physique des Solides.^{26,27} A monochromatic ^4He beam with energies ranging from 1.9 up to 2.2 MeV was used in the usual ERDA geometry (75° tilt of the samples). A 10 μm Mylar absorber was placed in front of the Si surface barrier detector, located at $\theta_{\text{lab}} = 30^\circ$, to stop the forward-scattered ^4He particles. Energy and composition calibrations were performed by means of totally hydrogenated, $(\text{C}_8\text{H}_8)_n$, and deuterated, $(\text{C}_8\text{D}_8)_n$, polystyrene thin film references prepared by spin-coating. These reference targets are stable enough under our experimental conditions to be used as standard targets for hydrogen quantitative analysis.²⁸ The H content of these samples was determined via their carbon content using the procedure described in ref 29. The stability of the silica samples was checked by means of a multichannel analyzer, indicating hydrogen losses always better than 5%.

Hydrogen Elimination Mechanisms

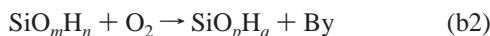
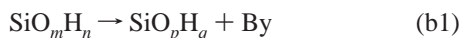
To define the framework for further discussion of our results, it is pertinent to give first a brief overview of the physicochemical mechanisms relevant to the hydrogen elimination process in the SiH_4/O_2 CVD system. Among them, we can distinguish the following four (see Figure 1).

(a) Production of Precursor Species and Radicals. On the basis of previous studies,^{8–15} the film is considered to grow predominantly through film precursor species (SiO_mH_n) formed in the gas phase, whereas direct adsorption and subsequent surface reactions of SiH_4 contributing to film deposition are supposed to be negligible. Film precursor species (SiO_mH_n) and H, O, OH, and HO_2 radicals (R) are produced simultaneously in the gas phase by the chain reactions described above, which can be synthesized as follows:



where By represents reaction byproducts (i.e., H_2 , H_2O , and H_2O_2). Note that reaction a1 stands for reactions 1–4, whereas reaction a2 includes reactions 5–7. The SiO_mH_n precursor species in reaction a2 could be of the form HSiOOH , H_2SiO , or H_3SiO .^{5–7}

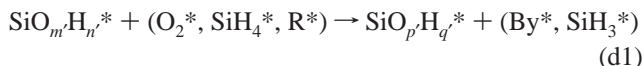
(b) Gas-Phase Elimination. Self-decomposition (b1), oxidation (b2), and reactions with SiH_4 molecules (b3) are considered to be the most plausible hydrogen elimination routes in the branching stage of SiH_4 oxidation:^{5,13,30–33}



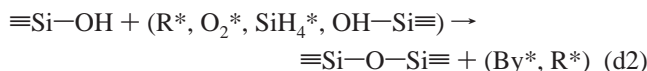
where SiO_pH_q represents a less hydrogenated species with $q < n$.

(c) Gas-Phase Diffusion. In a hot-wall, laminar regime CVD reactor, the mass transport in the gas phase is considered to be controlled by the diffusion of species, driven by concentration gradients, through a stagnant layer. Film precursor species (c1), radicals (c2), and O_2 (c3) and SiH_4 (c4) molecules diffuse through this stagnant layer from the gas stream to the film surface, where they can further adsorb and react as described below. In the same way, the adsorbed byproducts (By*) resulting from these surface reactions can desorb and diffuse through the stagnant layer toward the gas stream (c5).

(d) Surface Elimination. At present, the heterogeneous phenomena is the least understood issue in SiH_4 oxidation, in part due to the fact that most of the studies dealing with this reaction has been devoted to its gas-phase chemistry. However, our further discussion can be developed from two simple sets of surface reactions: dehydrogenation of SiO_mH_n^* species adsorbed on the film surface (d1) and of $\equiv\text{Si}-\text{OH}$ surface groups (d2). The first set may include self-decomposition, oxidation, reactions with SiH_4^* molecules, and reactions with H^* , O^* , OH^* , and HO_2^* radicals, yielding less hydrogenated species in the adsorbed state ($\text{SiO}_{p'}\text{H}_{q'}^*$, with $q' < n'$), adsorbed H_2O , H_2 , and H_2O_2 byproducts (By*), and SiH_3^* radicals in the case of reactions with SiH_4^* molecules:



The second set may include reactions of $\equiv\text{Si}-\text{OH}$ groups with incoming radicals (H^* , O^* , OH^* , and HO_2^*), O_2^* and SiH_4^* molecules, and adjacent $\equiv\text{Si}-\text{OH}$ groups (dehydroxylation reactions), to give byproducts (H_2O^* , H_2^* , and H_2O_2^*) and, possibly, additional radicals (e.g., OH^* or HO_2^*):



Those SiOH surface groups from which hydrogen is not eliminated and those hydrogenated species (intermediate precursors and byproducts) remaining adsorbed on the surface become finally buried by the growing film and thus incorporated into it. Thus, within the framework of this model, hydrogen elimination can be limited by any of the following mechanisms: gas-phase production of dehydrogenating radicals (a2), gas-phase elimination reactions (b1–b3), diffusion of dehydro-

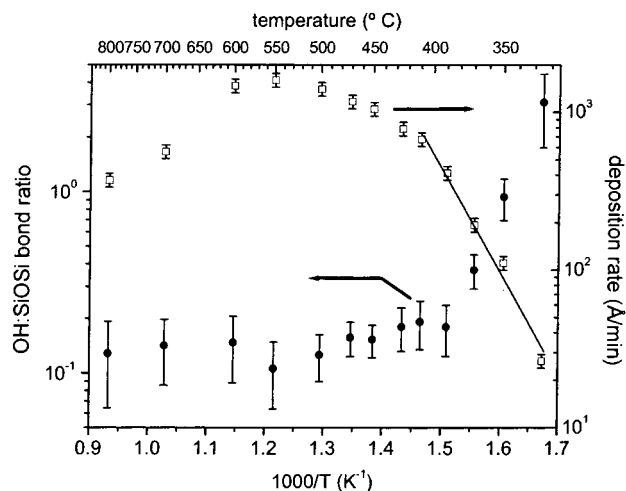


Figure 2. Arrhenius plots of deposition rate and OH:SiOSi bond ratio, as determined by IRS, for silica films deposited at $P = 1.4$ Torr, $F_T = 250$ sccm, and $[\text{O}_2]:[\text{SiH}_4] = 15$.

genating species (O_2 , SiH_4 , or radicals) toward the film surface (c2–c4), diffusion of adsorbed byproducts (H_2O^* , H_2^* , or H_2O_2^*) toward the gas stream (c5), or surface elimination reactions (within d1 or d2).

Results and Discussion

The mechanisms described above are discussed in this section according to the growth kinetics and influence of the experimental parameters (temperature, T , total gas flow rate, F_T , and oxygen-to-silane flow ratio, $[\text{O}_2]:[\text{SiH}_4]$) on the hydrogen concentration in the film (given by the OH:SiOSi bond ratio). The main goal is to identify the mechanisms limiting the hydrogen elimination process operating in the SiH_4/O_2 system, with the eventual purpose of concluding a simple kinetic model for this process.

Influence of Temperature. The influence of temperature on the deposition rate as well as on the resulting OH:SiOSi bond ratio in the films has been studied from experiments carried out at a pressure $P = 1.4$ Torr, total gas flow rate $F_T = 250$ sccm, and gas flow ratio $[\text{O}_2]:[\text{SiH}_4] = 15$. The results are shown in Figure 2, where the deposition rate and the OH:SiOSi bond ratio have been represented in Arrhenius-type plots. In the deposition rate plot we can distinguish three well-defined regions:¹⁵ an activated region between 325 and 400 °C, a weaker dependence region between 400 and 550 °C, and a decreasing region between 550 and 800 °C. The activated region in the low-temperature range was identified with a kinetically controlled process, with an apparent activation energy of (1.41 ± 0.2) eV. This activation energy was concluded to correspond to some elementary gas-phase reaction, included in the global reaction a2, where different SiO_mH_n intermediate species are produced (*gas-phase kinetic regime*). The weak T -dependence region was assigned to a *mass-transfer regime* (growth limited by step c1). The decreasing region was associated with the depletion of silane in the reaction zone, enhanced by the increase of temperature and by the progressive widening of the temperature profile along the reactor tube. The thermal pyrolysis of SiH_4 , yielding SiH_2 species, which becomes significant above 500 °C,^{7,31,34,35} could enhance these depletion effects and explain the sudden decrease of the deposition rate observed above 550 °C.

Figure 2 also shows that below ~ 420 °C the OH:SiOSi bond ratio increases abruptly with temperature, which means that hydrogen incorporation is being controlled by an activated

mechanism strongly dependent on temperature: e.g., gas-phase production of dehydrogenating radicals (a2), gas-phase elimination (b1–b3), or surface elimination reactions (d1 or d2). Taking into account the weak T -dependence of the gas-phase diffusion coefficients (typically $D_g \propto T^\alpha$, with $\alpha = 1.5–2$),³⁶ none of the gas-phase diffusion steps relevant to hydrogen elimination (c2–c5) is expected to control this process below 420 °C.

Above ~420 °C, the OH:SiOSi ratio is practically insensitive to temperature. In this case, hydrogen elimination could be limited either by mass transport (c2–c5 diffusion channels) or by a nonactivated (or low activation energy) reaction. In principle, either of the gas-phase or surface reactions described above could fulfill this condition, i.e., a2, b1–b3, d1, or d2.

ERDA was employed to study in more detail the hydrogen incorporation in the intermediate- and high-temperature ranges (390 °C < T < 800 °C), since above 500 °C the hydrogen content measured by IRS was very close to the detection limit of the spectrophotometer, i.e., the signal-to-noise ratio for the O–H band became very high. From the ERDA spectra we have obtained the H/Si atomic ratio of the film. The results, represented in Figure 3, reveal that the weak T -dependence regime for hydrogen elimination ends up around 470 °C. Beyond this temperature, the hydrogen concentration starts again to decrease abruptly with temperature, suggesting the beginning of a new regime for hydrogen elimination. This behavior may be related to the SiH₄ pyrolysis mentioned above, since the presence of SiH₂ species largely modifies the chemical path of SiH₄ oxidation.^{7,31} Accordingly, SiH₂ species could induce the formation of new precursor species with a lower hydrogen content in their formulas, and/or raise the gas-phase concentration of dehydrogenating radicals. However, the hydrogen depth profiles obtained from the ERDA spectra (see below) revealed a certain hydrogen accumulation at the outermost film surface for deposition temperatures just above 470 °C, which suggests a different explanation for this new regime.

ERDA spectra corresponding to films grown at 425, 470, 600, and 800 °C for 20 min are represented in Figure 4. The spectrum shape of the 425 °C film corresponds to a homogeneous depth concentration profile. For temperatures of 470 °C and higher, the spectra show a surface peak with increasing intensity up to 600 °C, and with decreasing intensity beyond this temperature. From the simulation of the 600 °C spectrum with the *senras* software,³⁷ the H/Si atomic ratio was deduced to be 0.630 at the film surface and 0.250 in the bulk. This hydrogen accumulation suggests that the buried hydrogen is able to diffuse through the film toward zones of low hydrogen concentration (film

surface and film/substrate interface) during the deposition experiment, although incompletely for its 20 min of duration (since the furnace was immediately removed from the reaction zone just after each deposition experiment, the sample temperature decreased to 400 °C in a few minutes and thus the time relevant to diffusion is close to 20 min in all cases). Hydrogen is also expected to accumulate at the SiO₂/Si interface, not observed in the ERDA spectra due to the high thickness of the films (>8000 Å).

Hydrogen diffusion in hydroxylated silica is generally described as the diffusion of H₂O molecules through a microporous material, a complex process involving –H migration by reactions between SiOH and SiOSi groups, reversible dehydroxylation reactions with ionic exchange, H₂O adsorption on chemically heterogeneous surfaces, capillary condensation, and bulk and surface H₂O migration.^{38–45} The overall diffusion process is enhanced by temperature, which results in an increasing hydrogen accumulation at the film surface up to 600 °C for 20 min of deposition. This effect competes with the decrease of the film thickness due to the lower deposition rate (see Figure 2), leading to a decreasing hydrogen accumulation above 600 °C. Therefore, at high temperatures ($T > 500$ °C), hydrogen bulk diffusion seems to influence the hydrogen concentration profile across the film for a given experiment time,

growth kinetic regimes. The deposition experiments were performed at temperatures of 370 and 410 °C (see Figure 5). The [O₂]:[SiH₄] flow ratio was fixed at 15 and total pressure at 1.4 Torr. For both temperatures, the deposition rate shows a maximum value for a given total gas flow rate, a behavior that is characteristic of CVD processes governed by gas-phase intermediate species.^{15,46,47} In the low- F_T region, the deposition rate is limited by the mass-transport rate (diffusion step c1), which increases with F_T as a consequence of the thinner stagnant layer through which the SiO_{*m*}H_{*n*} intermediate species must diffuse⁴⁸ (the stagnant layer thickness varies approximately as $F_T^{-1/2}$).⁴⁹

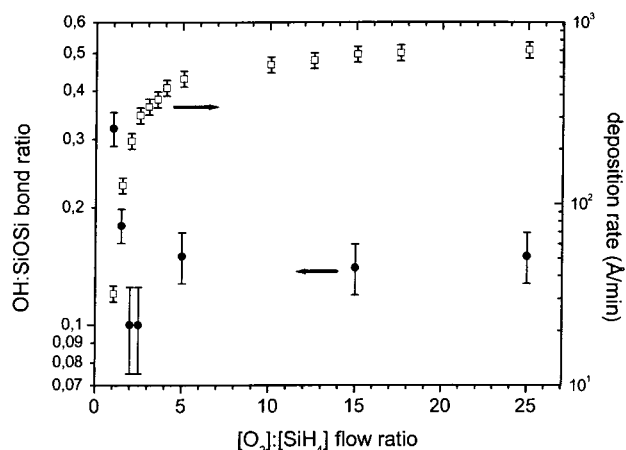


Figure 6. Influence of $[\text{O}_2]:[\text{SiH}_4]$ flow ratio on deposition rate and OH:SiOSi bond ratio, as determined by IRS, under the gas-phase kinetic regime ($F_T = 500$ sccm, $T = 450$ °C, and $P = 1.3$ Torr).

involved in hydrogen elimination (i.e., H_2O , H_2 , H_2O_2 , H , O , OH or HO_2 , O_2 , or SiH_4 species) diffuse faster than the SiO_mH_n precursor species, as expected from the lower molecular masses of the former. In any case, note that the diffusion of O_2 molecules from the gas phase to the film surface (c3) can be discarded as a limiting step for hydrogen elimination since the high $[\text{O}_2]:[\text{SiH}_4]$ flow ratio used in these experimental series ensures an excess of O_2 molecules at the film surface for the dehydrogenation of adsorbed SiO_mH_n species (d1) and/or SiOH surface groups (d2).

Influence of Oxygen-to-Silane Flow Ratio. To gain a deeper insight into the relevant mechanisms to hydrogen elimination, we have studied the influence of the $[\text{O}_2]:[\text{SiH}_4]$ ratio on the hydrogen concentration under the gas-phase kinetic regime. In the SiH_4/O_2 branching-chain reactions, there is a unique combination of O_2 and SiH_4 molar fractions for a given temperature and pressure for which the production of intermediate species is maximized.^{6,31,52–54} The SiO_mH_n production is reduced as the molar fraction of either O_2 or SiH_4 is increased or even completely inhibited when either of them is high enough.

Figure 6 shows the variation with the $[\text{O}_2]:[\text{SiH}_4]$ ratio of deposition rate and OH:SiOSi ratio at a high enough F_T (500 sccm) to allow us to operate under the gas-phase kinetic regime. The total pressure in the reactor was maintained at 1.3 Torr, and the temperature, at 450 °C. In this case, the SiH_4 molar fraction is practically constant as the $[\text{O}_2]:[\text{SiH}_4]$ flow ratio is varied, since O_2 flow variations are compensated mostly by N_2 flow variations when F_T is kept at constant value. Specifically, as the $[\text{O}_2]:[\text{SiH}_4]$ flow ratio increases from 1 to 25, the O_2 molar fraction (partial pressure) increases from 0.02 (25 mTorr) to 0.33 (433 mTorr), while SiH_4 molar fraction decreases from 0.019 (24.7 mTorr) to 0.013 (17.4 mTorr).

For $[\text{O}_2]:[\text{SiH}_4] < 5$, the deposition rate increases rapidly with the $[\text{O}_2]:[\text{SiH}_4]$ ratio, which means that the gas-phase production of film precursor species is determined by the O_2 molar fraction in the mixture. For $[\text{O}_2]:[\text{SiH}_4] > 5$, the increase of the deposition rate with the $[\text{O}_2]:[\text{SiH}_4]$ ratio is much slower, which denotes that the SiH_4 consumption tends to be maximized and that there is an excess of O_2 inhibiting the gas-phase reactions rather than contributing to the SiO_mH_n production. If the $[\text{O}_2]:[\text{SiH}_4]$ flow ratio were further increased, we would observe a decay of the deposition rate until reaching an upper critical limit above which the SiH_4/O_2 branching-chain reactions would be completely inhibited.^{3,8,9,55,56} Analogously, a lower critical limit around $[\text{O}_2]:[\text{SiH}_4] = 1$ below which the deposition rate vanishes can be observed in Figure 6.

The hydrogen concentration shows again a behavior practically opposite to that of deposition rate. For $[\text{O}_2]:[\text{SiH}_4] < 2$, the OH:SiOSi ratio decreases rapidly with increasing $[\text{O}_2]:[\text{SiH}_4]$ ratio, whereas for $[\text{O}_2]:[\text{SiH}_4] > 2$, it is nearly constant. When the O_2 molar fraction in the mixture is low, the production of the SiO_mH_n intermediate species in the gas phase (reaction a2) is also low, resulting in a low deposition rate. At the same time, the production of dehydrogenating radicals (a2) and the SiO_mH_n -into- SiO_pH_q conversion efficiency by gas-phase oxidation (b2) are low. Therefore, either of both mechanisms could limit hydrogen elimination under the gas-phase kinetic regime and explain the high concentration of SiOH groups found in the films for $[\text{O}_2]:[\text{SiH}_4] < 2$. By contrast, SiO_mH_n decomposition reactions (b1) are not expected to depend significantly on the O_2 molar fraction, and thus can be discarded as a limiting mechanism for hydrogen elimination under this regime. The same argument could be applied to dehydrogenation reactions of the type $\text{SiO}_m\text{H}_n + \text{SiH}_4 = \text{SiO}_m\text{H}_{n-1} + \text{SiH}_3 + \text{H}_2$ (b3), since the SiH_4 molar fraction remains practically unchanged, as mentioned above.

Mixtures richer in O_2 enhance the production of SiO_mH_n species and dehydrogenating radicals and facilitate the SiO_mH_n oxidation, being plausible explanations for the higher deposition rate and lower incorporation of SiOH groups into the film observed for higher $[\text{O}_2]:[\text{SiH}_4]$ ratios. For $[\text{O}_2]:[\text{SiH}_4] > 2$, the production of SiO_mH_n species tends to saturation. Therefore, the gas-phase production of dehydrogenating radicals, which is accompanied by the SiO_mH_n production in reaction a2, is also expected to be quite constant for $[\text{O}_2]:[\text{SiH}_4] > 2$, being a plausible candidate to control hydrogen elimination under the gas-phase kinetic regime. By contrast, while the SiO_mH_n production is maintained, the O_2 excess should make the gas-phase oxidation of these species more efficient. Therefore, the fact that the OH:SiOSi ratio is not significantly reduced for $[\text{O}_2]:[\text{SiH}_4] > 2$ allows us to reject the gas-phase oxidation of SiO_mH_n species (reaction b2) as a limiting factor for hydrogen elimination under the gas-phase kinetic regime.

Final Remarks. The above results support that, under the gas-phase kinetic growth regime, hydrogen elimination is limited by the gas-phase production of dehydrogenating radicals through reaction a2. In coherence, we expect the dehydrogenation of adsorbed SiO_mH_n species and $\equiv\text{Si}-\text{OH}$ groups by reactions with radicals colliding with the film surface to be the preferential path for hydrogen elimination in our system. Under the mass-transport growth regime, hydrogen elimination would be then limited by the diffusion either of these radicals toward the film surface (c2) or of the surface byproducts toward the gas-phase (c5).

A revealing trend common to the whole set of our results is that hydrogen concentration decreases with increasing deposition rate (see Figures 2, 5, and 6), which is inconsistent with hydrogen elimination models based on pure surface phenomena (like H_2O desorption or dehydroxylation reactions). Our kinetic model provides an evident explanation for this behavior by assuming that the flux of dehydrogenating radicals impinging on the growing film surface, which increases with deposition rate, is able to overcome the burying effect of the incident precursor species. This model is also compatible with previous observations on the SiH_4/O_2 chemistry. For instance, the heterogeneous quenching of the active radicals on the surface exposed to them (film surface and reactor walls) is known to be the dominant inhibition channel of SiH_4 oxidation at low pressures,³¹ which supports a hydrogen elimination model based on radical–surface interactions. In this regard, the SiOH surface

groups at the reactor walls have been reported to behave as radical termination sites that affect the lower critical limit of SiH₄ oxidation, leading to hysteresis phenomena when varying the deposition temperature in the 300–400 °C range due to variations of the wall hydroxylation degree between experiment and experiment.¹⁵ In addition, silica deposition from SiH₄/O₂ mixtures has been reported to occur predominantly through only one type of intermediate species (SiO_mH_n with *m* and *n* having unique values),¹¹ which is in agreement with a hydrogen elimination path lacking in gas-phase dehydrogenation reactions such as b1–b3. Neutral radicals are also known to play an important role in the growth and hydrogen elimination mechanisms involved in other CVD systems: e.g., hydrogen abstraction reactions in diamond^{57,58} and silicon^{59,60} CVD (with the application of different activation methods such as plasmas or hot filaments) and oxygen atom induced deposition of silica films⁶¹ in plasma-enhanced CVD from tetraethyl orthosilicate/O₂ mixtures. The specific surface mechanisms accounting for the hydrogen elimination process in our system, probably included in reactions d1 and d2, are beyond the scope of this work and would need extensive investigations at a fundamental level.

Summary and Conclusions

The mechanisms limiting the hydrogen elimination process in chemical vapor deposition of silica films obtained from SiH₄/O₂ mixtures have been investigated. Our results suggest that the film grows through intermediate SiO_mH_n species diffusing toward the film surface, where they adsorb and further incorporate, yielding SiOH surface groups. Simultaneously, dehydrogenating radicals (H, O, OH, and HO₂) produced in the gas phase by means of the same reactions diffuse to the film surface, where they adsorb and further eliminate hydrogen from adsorbed species (e.g., SiO_mH_n molecules and/or ≡SiOH groups). We have found a clear correlation between the growth and hydrogen elimination kinetics. When the film growth is limited by the gas-phase kinetics, which is attained at low temperatures and/or high total gas flow rates, hydrogen elimination is limited by the gas-phase production of dehydrogenating radicals. Likewise, when the growth is limited by the mass-transport rate, the regime that operates at intermediate/high temperatures and/or low total gas flow rates, hydrogen elimination is limited either by the diffusion of these radicals toward the film surface or by the diffusion of surface byproducts (H₂, H₂O, or H₂O₂ molecules) toward the gas stream. At very high temperatures (>470 °C), bulk diffusion of hydrogenated species trapped by the growing film causes a certain hydrogen accumulation at the film surface and probably at the film/substrate interface for a given experiment time.

Acknowledgment. This work was partially supported by the ECSC 7220-ED/082 project and by the 07M/0710/97 project from Comunidad Autónoma de Madrid (CAM). F.O. also gratefully acknowledges the grant financed by CAM (683/96, BOCM 22/4/96).

References and Notes

- Jensen, K. F.; Kern, W. In *Thin Film Processes II*; Vossen, J. L., Kern, W., Eds.; Academic Press: Boston, 1991.
- Lakhani, A. A. *Solid-State Electronics* **1984**, *27*, 921.
- Bennett, B. R.; Lorenzo, J. P.; Vaccaro, K. *Appl. Phys. Lett.* **1987**, *50*, 197.
- Katz, A.; Feingold, A.; Chakrabarti, U. K.; Pearton, S. *J. Appl. Phys. Lett.* **1991**, *59*, 2552.
- Hartman, J. R.; Famil-Ghiriha, J.; Ring, M. A.; O'Neal, H. E. *Combust. Flame* **1987**, *68*, 43.
- Kondo, S.; Tokuhashi, K.; Nagai, H.; Iwasaka, M.; Kaise, M. *Combust. Flame* **1995**, *101*, 170.
- Koda, S.; Fujiwara, O. *Proc. Symp. Int. Combust., 21st* **1986**, 1861.
- Vasilyeva, L. L.; Drozdov, V. N.; Repinsky, S. M.; Svitashov, K. *Thin Solid Films* **1978**, *55*, 221.
- Taft, E. A. *J. Electrochem. Soc.* **1979**, *126*, 1728.
- Vasiliev, Y. V.; Vasilieva, L. L.; Drozdov, V. N.; Shklyayev, A. *Thin Solid Films* **1981**, *76*, 61.
- Watanabe, K.; Komiyama, H. *J. Electrochem. Soc.* **1990**, *137*, 1222.
- Liehr, M.; Cohen, S. A. *Appl. Phys. Lett.* **1992**, *60*, 198.
- Takahashi, T.; Hagiwara, K.; Egashira, Y.; Komiyama, H. *J. Electrochem. Soc.* **1996**, *143*, 1355.
- van de Weijer, P.; Zwerver, B. H. *Chem. Phys. Lett.* **1989**, *163*, 48.
- Ojeda, F.; Castro-García, A.; Gómez-Aleixandre, C.; Albella, J. M. *J. Mater. Res.* **1998**, *13*, 2308.
- Pliskin, W. A.; Lehman, H. S. *J. Electrochem. Soc.* **1965**, *112*, 1013.
- Lange, P.; Shnakenerg, U.; Ullerich, S.; Schliwinski, H.-J. *J. Appl. Phys.* **1990**, *68*, 3532.
- Najmi, O.; Montero, I.; Galán, L.; Perrière, J.; Albella, J. M. *Appl. Surf. Sci.* **1993**, *70/71*, 217.
- Montero, I.; Galán, L.; Najmi, O.; Albella, J. M. *Phys. Rev. B* **1994**, *50*, 4881.
- Han, S. M.; Aydil, E. S. *Thin Solid Films* **1996**, *290–291*, 427.
- Goulet, A.; Charles, C.; García, P.; Turban, G. *J. Appl. Phys.* **1993**, *74*, 6876.
- Griscom, D. L. *MRS Bull.* **1987**, June 16/August 15, 20.
- Ferendeci, A. M. *Physical Foundations of Solid State and Electron Devices*; McGraw-Hill: New York, 1991.
- Ojeda, F.; Montero, I.; Abel, F.; Albella, J. M. *Chem. Mater.* **2001**, *13*, 3986.
- Adams, A. C.; Alexander, F. B.; Capio, C. D.; Smith, T. E. *J. Electrochem. Soc.* **1981**, *128*, 1545.
- Amsel, G.; Nadai, J. P.; d'Artemare, E.; David, D.; Girard, E.; Moulin, J. *Nucl. Instrum. Methods* **1971**, *92*, 481.
- Chu, W. K.; Mayer, J. W.; Nicolet, M.-A.; Buck, T. M.; Amsel, G. *Thin Solid Films* **1973**, *17*, 1.
- Abel, F.; Quillet, V.; Schott, M. *Nucl. Instrum. Meth. B* **1995**, *105*, 86.
- Quillet, V.; Abel, F.; Schott, M. *Nucl. Instrum. Meth. B* **1993**, *83*, 47.
- Kondo, S.; Tokuhashi, K.; Nagai, H.; Takahashi, H.; Kaise, M.; Sugie, M.; Aoyagi, M.; Mogi, K.; Minamino, S. *J. Phys. Chem. A* **1997**, *101*, 6015.
- Koda, S. *Prog. Energy Combust. Sci.* **1992**, *18*, 513.
- Aivazyan, R. G. *Kinet. Catal.* **1997**, *38*, 174.
- Aivazyan, R. G.; Sinel'nikova, T. A. *Kinet. Catal.* **1994**, *35*, 17.
- Han, J. H.; Rhee, S. W.; Moon, S. H. *J. Electrochem. Soc.* **1996**, *143*, 1996.
- Bell, T. N.; Perkins, K. A.; Perkins, P. G. *J. Phys. Chem.* **1984**, *88*, 116.
- Morosanu, C. E. *Thin Films by Chemical Vapor Deposition. In Thin Films Science and Technology*, 7; Elsevier: Amsterdam, 1990.
- Vizkelethy, G. *Nucl. Instrum. Methods B* **1990**, *45*, 1.
- Shackelford, J. F.; Masaryk, J. S. *J. Non-Cryst. Solids* **1976**, *21*, 55.
- Rosencher, E.; Straboni, A.; Rigo, S.; Amsel, G. *Appl. Phys. Lett.* **1979**, *34*, 254.
- Pfeffer, R.; Ohring, M. *J. Appl. Phys.* **1981**, *52*, 777.
- Mikkelsen, J. C., Jr. *Appl. Phys. Lett.* **1984**, *45* (11), 1187.
- Li, S. C.; Muraka, S. P. *J. Appl. Phys.* **1992**, *72*, 4214.
- McGinnis, P. B.; Shelby, J. E. *J. Non-Cryst. Solids* **1994**, *179*, 185.
- Poindexter, E. H. *J. Non-Cryst. Solids* **1995**, *187*, 257.
- Doremus, R. H. *J. Mater. Res.* **1995**, *10*, 2379.
- Kamata, K.; Maruyama, K.; Amano, S.; Fukazawa, H. *J. Mater. Sci. Lett.* **1990**, *9*, 316.
- Ellis, F. B.; Gordon, R. G. *J. Appl. Phys.* **1983**, *54*, 5381.
- Hampden-Smith, M.; Kodas, T. T. *Chem. Vap. Deposition* **1995**, *1*, 8.
- Kern, W., In *Microelectronic Materials and Processes*; Levy, R. A., Ed.; NATO ASI Series E; Kluwer Academic Publishers: Dordrecht, 1986; Vol. 164, p 203.
- Weiller, B. H. *J. Mater. Res. Soc. Symp. Proc.* **1994**, *334*, 379.
- Keyser, L. F. *J. Phys. Chem.* **1984**, *88*, 4750.
- Emelús, H. J.; Stewart, K. *J. Chem. Soc. (London)* **1935**, 1182.
- Emelús, H. J.; Stewart, K. *J. Chem. Soc. (London)* **1936**, 677.
- Azatyan, V. V.; Aivazyan, R. G. *Kinet. Catal.* **1991**, *32*, 1149.
- Cobianu, C.; Pavelescu, C. *J. Electrochem. Soc.* **1983**, *130*, 1888.
- Graham, J. *High Temperatures—High Pressures* **1974**, *6*, 577.
- Butler, J. E.; Woodin, R. L. *Philos. Trans. R. Soc. London A* **1993**, *342*, 209.
- Angus, J. C.; Wang, Y.; Sunkara, M. *Annu. Rev. Mater. Sci.* **1991**, *21*, 221.
- Kratzer, P. *J. Chem. Phys.* **1997**, *106*, 6752.
- Nakajima, K.; Miyazaki, K.; Koinuma, H.; Sato, K. *J. Appl. Phys.* **1998**, *84*, 606.
- Raup, G. B.; Cale, T. S.; Hey H. P. W. *J. Vac. Sci. Technol. B* **1992**, *10*, 37.